

Orbital volume measurements from magnetic resonance images using the techniques of manual planimetry and stereology

ABSTRACT

Introduction: Current volume measurement techniques, for the orbit, are time-consuming and involve complex assessments, which prevents their routine clinical use. In this study, we evaluate the applicability and efficacy of stereology and planimetry in orbital volume measurements using magnetic resonance imaging (MRI).

Materials and Methods: Prospective imaging study using MRI. Sheep craniums and human subjects were evaluated. Water-filling measurements were performed in animal skulls, as the standard validation technique. Planimetry and stereology techniques were used in each dataset. Intraobserver and interobserver reliability testing were applied.

Results: In stereology customization, 1/6 systematic sampling scheme was determined as optimal with acceptable coefficient of error (3.09%) and low measurement time (1.2 min). In sheep craniums, the mean volume measured by water displacement, planimetry, and stereology was $17.81 \pm 0.59 \text{ cm}^3$, $18.53 \pm 0.24 \text{ cm}^3$, and $19.19 \pm 0.17 \text{ cm}^3$, respectively. Planimetric and stereological methods were highly correlated ($r = 0.94$; $P < 0.001$). The mean difference of the orbital volume using planimetry and stereology was $0.316 \pm 0.168 \text{ cm}^3$. In human subjects, using stereology, the mean orbital volume was found to be $19.62 \pm 0.2 \text{ cm}^3$ with a CE of $3.91 \pm 0.15\%$.

Conclusions: The optimized stereological method was found superior to manual planimetry in terms of user effort and time spent. Stereology sampling of 1/6 was successfully applied in human subjects and showed strong correlation with manual planimetry. However, optimized stereological method tended to overestimate the orbital volume by about 1 cc, a considerable limitation to be taken in clinical practice.

Keywords: Eye, orbit, planimetry, skull, stereology

INTRODUCTION

Quantitative measurements of the orbital cavity are essential for understanding and monitoring orbital disease. Orbital volume, in particular, is valuable in clinical practice for managing orbital pathologies such as maxillofacial trauma,^[1] orbital tumors,^[2,3] and congenital deformities.^[4] Accurate preoperative assessment of the orbital contents is crucial for achieving anatomically desirable outcomes.^[5] Recent advances in three-dimensional (3D)-printing technology have enabled customized orbital reconstruction, using accurately designed implants.^[6]


Traditionally, computed tomography (CT) imaging is the modality of choice for assessing the osseous elements of

GEORGIOS BONTZOS, MICHAEL MAZONAKIS¹, EFROSINI PAPADAKI², THOMAS G. MARIS¹, STYLIANI BLAZAKI, ELENI E. DRAGONAKI³, EFSTATHIOS T. DETORAKIS

Department of Ophthalmology, University Hospital of Heraklion,
³Independent Imaging Services, Heraklion, Crete, ¹Department of Medical Physics, University of Crete, ²Department of Radiology, University Hospital of Heraklion, Heraklion, Greece

Address for correspondence: Dr. Georgios Bontzos, Department of Ophthalmology, University Hospital of Heraklion, 71110, Stavrakia, Heraklion, Crete, Greece.
 E-mail: gbontzos@hotmail.gr

Received: 29 January 2020, **Revised:** 08 May 2020,
Accepted: 15 May 2020, **Published:** 18 June 2020

Access this article online	
Website: www.njms.in	Quick Response Code 
DOI: 10.4103/njms.NJMS_9_20	

This is an open access journal, and articles are distributed under the terms of the Creative Commons Attribution-NonCommercial-ShareAlike 4.0 License, which allows others to remix, tweak, and build upon the work non-commercially, as long as appropriate credit is given and the new creations are licensed under the identical terms.

For reprints contact: WKHLRPMedknow_reprints@wolterskluwer.com

How to cite this article: Bontzos G, Mazonakis M, Papadaki E, Maris TG, Blazaki S, Drakonaki EE, *et al.* Orbital volume measurements from magnetic resonance images using the techniques of manual planimetry and stereology. *Natl J Maxillofac Surg* 2020;11:20-7.

the orbit.^[7] On the contrary, soft tissue structures such as the extraocular muscles, orbital fat, and the optic nerve are optimally visualized using magnetic resonance imaging (MRI).^[8] The described limitations force patients to undergo several imaging examinations for proper evaluation and datasets then require complex postprocessing algorithms which allow fusing and cumulative measurements.^[9,10]

Several methods have been described to measure the orbital volume and validate the respective measurements.^[11-16] Nevertheless, the vast majority of these studies were tested only on CT datasets and the proposed methodologies required manual segmentation of the orbital cavity. A single measurement of the desired area may require several hours, while the results are interobserver sensitive and can vary up to 15% between expert users.^[17] Currently, two main approaches can be used to assess the volume of the orbit: planimetry and stereology. Planimetry is considered the 'gold standard' reference technique and is based on the summation of the manually delineated areas obtained from a CT or MRI dataset. Stereology is based on statistical point-counting, based on the Cavalieri's principle, which states that the volume of an object can be calculated using its two-dimensional parallel sections, separated by a certain distance.^[18,19] For instance, volume measurements can be obtained from an organ of interest after cutting it from end-to-end starting at a random position and continuing on a set of equally spaced parallel section planes.^[20,21] In our previous work,^[22] we described the validity and repeatability of a semi-automated technique based on stereology for measuring the orbital volume on CT datasets. To the best of our knowledge, no previous work on the field has addressed the issue of computing the orbital volume on MRI by comparing both planimetry and stereology.

The presented study aims to provide a comprehensive analysis of the validity and reliability of orbital volume measurements derived using MRI datasets, using stereology and planimetry, and to compare the obtained results between the two methods.

MATERIALS AND METHODS

Study design

This is an experimental animal study based on MRI of sheep craniums. The applicability of the quantitative methods was then tested in human subjects. All the experimental animal procedures followed the ARVO statement for the Use of Animals in Ophthalmic and Vision Research and the institutional guidelines. The study was approved by local ethics committee and adhered to the tenets of the Declaration of Helsinki. The purpose of this study was explained to all participants, who gave signed written informed consent.

Study population

Five sheep heads (total of 10 orbits) were provided by the animal house of the University of Crete, Faculty of Medicine. Sheep were sacrificed on the same day as imaging and water-filling experiments. Afterward, the imaging quantification process was performed in five human subjects who were referred to the Department of Radiology of the University Hospital of Heraklion for orbital MRI, following symptoms of unidentified blurry vision, and were diagnosed as disease-free in the orbits and the periorbital area.

Image acquisition

In each subject, 3D-MRI was performed. MRI was performed using a clinical 1.5T whole-body superconducting imaging system (MAGNETOM Sonata/Vision, Siemens Healthcare, Erlangen, Germany), equipped with high-performance gradients (Gradient strength: 40 mT/m, Slew rate: 200 mT/m/ms) utilizing a standard circular polarized body coil as a transmitter and a linear polarized head coil as a receiver. The comprehensive MRI protocol consisted of one 3D T1w sequence [(3D-VIBE) (volume-interpolated breath-hold examination)] and one 3D (T2/T1) w sequence (3D-constructive interference on the steady state). Human subjects were instructed to keep both eyes closed with minimal movement during the scanning. The image resolution voxel was 1 mm × 1 mm × 1 mm. Axial, coronal, and sagittal images were obtained. The same imaging protocol was applied for the sheep craniums and for human subjects. The 3D-VIBE sequence was selected for measurements as it provides the best overall image quality^[23] and has been evaluated for osseous tissue abnormalities.^[24]

Exenteration of the animal eye socket/surgical technique

Following MRI, each orbit was carefully dissected to remove all soft tissue from the orbital cavity following standard enucleation procedure [Figure 1a]. The entire orbital contents were removed *en bloc* to the optic canal. Orbital soft tissue, extraocular muscles, and the orbital fat were removed. The globe and the optic nerve were isolated separately [Figure 1b]. The jugular and oval foramen were then sealed using clay.

Water-filling method

The anterior boundary of the orbit was determined as the line that connects the two endpoints of the front medial and lateral wall. The skull was immobilized in a way that the anterior boundary was perfectly horizontal. The orbital socket [Figure 1c] was filled with water to measure the orbital volume by calculating the quantity of the required fluid. These measurements served as a reference standard for volumetry calculations based on MRI.

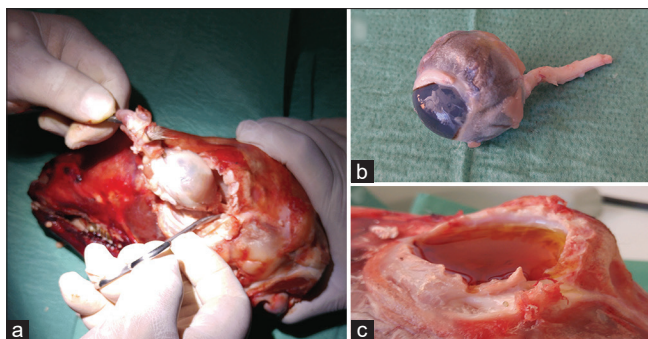


Figure 1: (a) Standard enucleation procedure of the soft tissue from the orbital cavity. The entire orbital contents were removed *en bloc* down to the optic canal. (b) The optic nerve was dissected from the canal part at the optic foramen and was isolated with the eye globe. (c) The orbital socket was immobilized in a perfectly horizontal direction. Then it was filled with water to measure the exact orbital volume

Planimetry technique

DICOM images from each dataset were exported to the open-source imaging processing software 3D Slicer v. 4.8.1, for image segmentation [Figure 2a], by applying manual 3D volume rendering [Figure 2b]. The orbit boundaries were manually delineated in axial slices. The area of the orbital cavity (a) was measured in each slice (i) and the sum was multiplied by slice thickness (T) to determine the total volume (V) of each orbit as shown in Eq. 1:

$$V = \sum_i^m (T a_i)$$

Stereology technique

Stereological orbital volume measurements were performed using the Analyze software (Mayo Foundation, Rochester, MN, USA). Stereology, as mentioned above, is a mathematical approach for volume measurements based on Cavalieri's principle, which involves systematic random sampling through the region of interest. Instead of tracing the region, selected sampling points over the region of interest are marked. Every point has a given area associated with it (A). The area of the organ of interest in a given section is the area of the total number of points selected by the user in our image dataset a square systematic array of test points was overlaid in each cross-section. Thereafter, all points lying within the area of the orbital cavity were selected by the user and the software automatically calculated the total number of point counts [Figure 2c]. The total volume (V) was given by Eq. 2:

$$V = TA \sum_i^m (p_i)$$

where m is the number of the sections depicting the orbit and P_i is the number of points lying within the orbital cavity on section i and T is the interval between the MR sections.

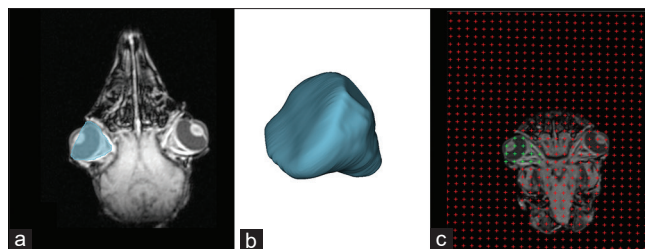


Figure 2: (a) Manual delineation of the orbital cavity on axial slicer by applying three-dimensional volume rendering in three-dimensional Slicer. (b) Three-dimensional model of the segmented orbit for measuring its total volume. (c) Stereological measurement of the orbital volume using the analyze software. A grid is placed over the slice and the green points which lie within the orbit are selected by the user. The total volume is then estimated based on the total number of point counts

The precision of stereological object volume estimation may be determined by its coefficient of error (CE) as reported by Gundersen and Jensen.^[20] The point spacing of the grid may be given by Eq. 3:

$$d = \sqrt{\frac{V}{N \cdot T}}$$

where V is an approximation of the volume of interest, N is the total number of counted points, and T is the interval between two consecutive sections used for stereological estimations. It is recommended that about 100–200 point counts may provide efficient stereological estimations.^[19] Therefore, volume estimations were also performed by selecting 150 test points in all sections. The distance d in Eq. 3 was found using an $n = 150$ points.

Stereology sampling and optimization

The stereological method enables the assessment of any organ volume together with its CE using only a sample of slices containing the organ of interest. Previous studies have indicated the efficiency of systematic slice sampling for volumetric analysis.^[25,26] Gundersen and Jensen^[20] reported that a CE of 5% is sufficient in stereological studies. To optimize the stereological technique, we randomly selected the right orbit of the third skull and we performed several estimations. We used sampling intensities of 1/2, 1/3, 1/4, 1/5, 1/6, 1/8, 1/10, and 1/12. One of these samples was randomly chosen for orbital volume estimation.

Imaging in human subjects

The same imaging protocol was used to obtain MRI datasets from five human subjects. Postprocessing analysis included orbital segmentation [Figure 3a] and quantification using planimetry [Figure 3b] and stereology [Figure 3c] as described above. CE of error was also reported to evaluate the performance of stereology in human orbits.

Statistical analysis

Statistical analysis was performed using SPSS for Windows, software version 22.0 (SPSS, Chicago, IL, USA). Distributions of quantitative variables were described as means (\pm standard deviation). All *P* values related to two-sided tests with a significance level of $\alpha = 0.05$. A nonparametric Mann–Whitney test was used to detect differences between groups. To test the proportion of agreement among measurements, we tested intraobserver and interobserver agreement as follows:

Intraobserver reliability of MRI measurements was calculated by comparing two separate measurements performed by one observer 1 month apart to minimize recall bias.

Interobserver reliability of MRI measurements was calculated by comparing computed volume estimations of two separate observers, using the same methodology. Both observers were experienced in orbital MRI and MR-based volumetry.

The intraclass correlation coefficient (ICC) (two-way mixed model) was computed to estimate interrater and intrarater

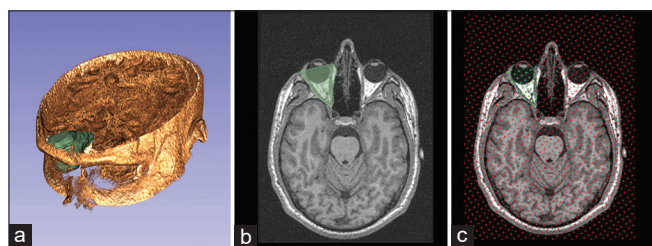


Figure 3: (a) Model of the segmented orbit within the human skull on three-dimensional Slicer. (b) Manual delineation of the orbital cavity on an axial magnetic resonance imaging slice, to be used for manual planimetry measurement. (c) Stereological technique, using 1/6 sampling for calculating the orbital volume based on the selected point count

reliability. An ICC value of >0.7 in absolute single measures was considered as an acceptable agreement. Correlations between measurements from planimetry, stereology, and water displacement experiments were examined by calculating the Pearson's correlation coefficient. Furthermore, a paired samples *t*-test was applied to identify significant differences in the mean values of the computed volumes.

Graphic displays were illustrated using GraphPad Prism (GraphPad Software Inc., La Jolla, CA, USA).

RESULTS

Water displacement experiments

In total, 10 orbits in sheep craniums were measured. The volume measured by the water displacement technique ranged between 16.82 cm³ and 18.59 cm³, while the mean orbital volume measured was 17.81 \pm 0.59 cm³ [Tables 1 and 2].

Definition of the optimal stereological sampling

In all cases, the entire orbit was depicted in 36–38 MRI slices. The precision of the obtained stereological orbital volume estimations is presented in Table 3. It was found that calculations resulted in CE of more than 5% when sampling intensities of 1/8 or more were adopted. Volume measurement on the entire slice set depicting an orbital cavity (38 slices) resulted in a CE of 0.55%. The 1/6 sampling intensity resulted in an acceptable 3.09% CE with 1.2 min measurement time. When compared with the actual volume of the orbit, as obtained by the water displacement method, the 1/6 sampling displayed a percentage difference of 3.01% compared to 1.34% for the entire dataset measurement (1/1

Table 1: Orbital volume planimetry measurements

Orbital cavity	Investigator 1 First measurement (cm ³)	Investigator 1 Second measurement (cm ³)	Investigator 2 Measurement (cm ³)	Mean value in planimetry (cm ³)	Intrapersonal difference (cm ³)	Interpersonal difference (cm ³)	Water displacement (gold standard)
Model 1							
Left orbit	18.91	18.98	18.72	18.87	0.07	0.19	18.12
Right orbit	18.64	18.82	18.93	18.79	0.18	0.29	17.86
Model 2							
Left orbit	18.36	18.51	18.64	18.50	0.15	0.28	17.53
Right orbit	18.25	18.42	18.37	18.34	0.17	0.12	17.74
Model 3							
Left orbit	19.25	19.33	19.82	19.47	0.08	0.57	18.45
Right orbit	19.46	19.17	19.28	19.30	0.29	0.18	18.59
Model 4							
Left orbit	19.03	18.81	18.95	18.93	0.22	0.08	18.13
Right orbit	18.83	18.79	18.74	18.79	0.04	0.09	18.04
Model 5							
Left orbit	17.22	17.39	17.25	17.29	0.17	0.03	16.82
Right orbit	17.34	17.51	17.97	17.61	0.17	0.63	16.90

Table 2: Orbital volume stereology measurements

Orbital cavity	Investigator 1 First measurement (cm ³)	Investigator 1 Second measurement (cm ³)	Investigator 2 Measurement (cm ³)	Mean value in stereology (cm ³)	Intrapersonal difference (cm ³)	Interpersonal difference (cm ³)	Water displacement (gold standard)
Model 1							
Left orbit	19.28	19.16	19.25	19.23	0.12	0.03	18.12
Right orbit	18.53	18.59	18.60	18.57	0.06	0.07	17.86
Model 2							
Left orbit	18.86	18.81	18.77	18.86	0.05	0.09	17.53
Right orbit	18.99	18.97	18.89	18.81	0.02	0.10	17.74
Model 3							
Left orbit	19.26	19.31	19.31	19.29	0.05	0.05	18.45
Right orbit	19.94	19.94	19.88	19.92	0.00	0.06	18.59
Model 4							
Left orbit	19.49	19.44	19.52	19.48	0.05	0.03	18.13
Right orbit	19.31	19.31	19.35	19.32	0.00	0.04	18.04
Model 5							
Left orbit	17.77	17.77	17.67	17.74	0.00	0.10	16.82
Right orbit	17.89	17.78	17.81	17.83	0.11	0.08	16.90

Table 3: Stereological orbital optimization/Model 3 - right orbit

Sample type	Number of measured slices	Sectioning thickness (T) (mm)	Measured volume (cm ³)	CE (%)	Measurement time (mins)
1/1	38	1	19.34	0.55	5.7
1/2	19	2	18.93	0.91	3.4
1/3	12	3	19.85	1.23	2.2
1/4	9	4	19.46	2.01	1.7
1/5	7	5	19.13	2.35	1.4
1/6	6	6	19.03	3.09	1.2
1/8	4	8	21.81	6.32	0.9
1/10	3	10	23.24	8.15	0.6

CE: Coefficient of error

sampling). Based on the above, measurements by stereology with 1/6 of the total slices was the considered the optimal approach. By following this method, measurements on animal skulls and human subjects were performed.

Image volumetry in animal models

Using planimetry [Table 1], the first investigator reported mean orbital volume of 18.53 ± 0.24 cm³ in the first and 18.57 ± 0.21 cm³ in the second evaluation, which was not significantly different ($P = 0.891$, paired samples *t*-test). Furthermore, the ICC showed high intrarater agreement (ICC = 0.985, $P \approx 0.001$). In addition, the second investigator measured a mean orbital volume of 18.67 ± 0.22 cm³, which was also not statistically significant compared with the first evaluation of the first investigator ($P = 0.677$, paired samples *t*-test) and displayed an excellent inter-rater agreement (ICC = 0.952; $P \approx 0.001$). The average measurement time for each data set was 21.3 min.

Using stereology sampling of 1/6 [Table 2] as described above, the first investigator reported the mean orbital volume of 19.19 ± 0.17 cm³ (CE = $3.54 \pm 0.39\%$) in the first and 19.17 ± 0.16 cm³ (CE = $4.13 \pm 0.27\%$) in the second evaluation,

which was not significantly different ($P = 0.462$, paired samples *t*-test). Furthermore, the ICC showed an excellent intrarater agreement (ICC = 0.995; $P \approx 0.001$). In addition, the second investigator reported a mean orbital volume of 19.17 ± 0.17 cm³ (CE = $3.14 \pm 0.18\%$) in his assessment, which was also not statistically significant compared with the first evaluation of the first investigator ($P = 0.503$, paired samples *t*-test), and a high interrater agreement was found in ICC (ICC = 0.995; $P \approx 0.001$).

To compare the different methods, we correlated the imaging measurements from the first measurement of the first investigator with the reference water-filling method. Volumes obtained by stereology were highly correlated with the water-filling method ($r = 0.939$; $P = 0.001$), while paired samples *t*-test yielded a statistically significant difference between the mean volumes computed by the water-filling method and stereology ($t = 14.38$; $P \approx 0.001$). Similarly, planimetry results also displayed high correlation with the water-filling method ($r = 0.98$; $P \approx 0.001$) and paired samples *t*-test revealed a significant difference ($t = 12.09$; $P = 0.001$). Finally, between

planimetry and stereology, a strong correlation was also noted ($r = 0.94$; $P \approx 0.001$) and a paired t -test displayed a statistically significant difference in mean values ($t = 4.936$; $P = 0.01$).

Image volumetry in human subjects

The same methods using planimetry and stereology were applied to estimate the orbital volume in five healthy subjects (10 total orbits). The measured volumes by planimetry [Figure 3b] ranged between 18.54 cm³ and 20.67 cm³, while the mean orbital volume was 19.61 ± 0.21 cm³. Using stereology sampling of 1/6 [Figure 3c], the estimated volume ranged between 18.57 cm³ and 20.52 cm³, and the mean orbital volume was found to be 19.62 ± 0.2 cm³ with a CE of 3.91 ± 0.15% [Table 4]. The mean measurement time for stereology was 2.4 ± 0.2 min. Total volumes obtained by planimetry were highly correlated with the those obtained from stereology ($r = 0.862$; $P = 0.001$, Pearson's correlation coefficient).

DISCUSSION

In this work, we evaluated the applicability of both planimetry and stereology for obtaining precise measurements of the orbital volume using MR datasets. First, we tested their performance in sheep craniums by comparing the results over water filling, as a reference standard. Both techniques yielded significant correlation with the water-filling method, $r = 0.98$ for planimetry and $r = 0.939$ for stereology. We also optimized stereological calculation process in order to minimize measurement time. For this reason, we choose the 1/6 sampling which resulted in acceptable CE of 3.09% while

measurements took an average of 1.2 min. Supplementary analysis using Bland–Altman plots [Figure 4] showed that planimetry tends to overestimate the orbital volume with an

Table 4: Orbital volume measurements in human subjects

Orbital cavity	Volume measured by planimetry (cm ³)	Volume measured by stereology (cm ³)	Stereology CE (%)
Subject 1			
Left orbit	19.54	19.62	4.27
Right orbit	19.23	19.43	3.53
Subject 2			
Left orbit	20.10	20.52	3.87
Right orbit	20.67	20.32	3.31
Subject 3			
Left orbit	19.25	19.66	3.71
Right orbit	19.74	19.32	4.24
Subject 4			
Left orbit	19.85	20.13	3.76
Right orbit	20.32	19.87	4.31
Subject 5			
Left orbit	18.54	18.79	4.87
Right orbit	18.77	18.57	3.29

CE: Coefficient of error

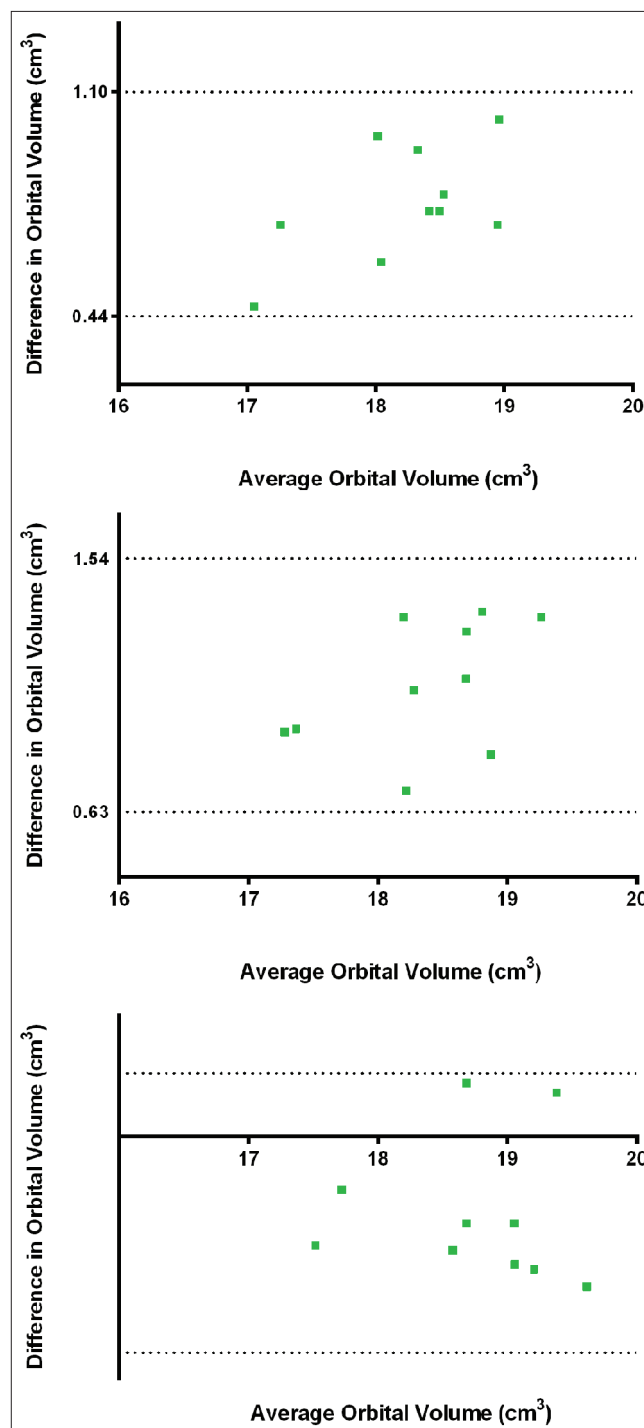


Figure 4: Bland–Altman plots for comparisons between methods. Upper plot: Differences in orbital volume estimates as defined by manual planimetry and the water-filling method. The mean difference is presented with the solid line whereas the 95% limits of agreement are shown with the dotted lines. Middle plot: Differences in orbital volume estimates as defined by the optimized stereological approach and the water-filling method. Lower plot: Differences in orbital volume measurement as defined by manual planimetry and stereology

average of 0.771 cm³, while stereology also overestimated the orbital volume by 1.087 cm³. Moreover, we tested the comparative performance of planimetry and stereology. The two methods displayed a strong correlation ($r = 0.94$). The imaging methods were also later applied in human subjects. Similarly, the two methods were highly correlated ($r = 0.862$).

The presented approach was similar to our previous work^[22] on CT datasets. Our results were in general agreement with those obtained from planimetry and stereology on CT in terms of applicability and CE; however, it was observed that calculations on MRI tend to overestimate the orbital volume by 4.32% using planimetry and 6.18% using stereology. At the same time, on CT scans of the same subjects, planimetry slightly overestimated the real orbital volume by 0.6% while stereology underestimated the volume by 1.46%. The above percentages are important since the precise evaluation of the volume is crucial for guiding clinical decisions. In fact, small changes in volume can lead to severe exophthalmos and ocular motility defects.^[15,27] It has been estimated that a 1 cm³ increase in orbital volume will result in 1 mm of axial displacement of the globe.^[28,29] The described limitations in calculations should especially be considered during surgical planning for orbital decompression procedures or for restoration of the orbit following trauma. Regardless of the approach or choice of materials, restoration of orbital volume to improve function should be the main goal of surgery.^[30] Apparently, the ability to accurately determine orbital volume could provide useful information in customized orbital implants.

It should be noted that orbital volume measurements are also remarkably useful for the understanding of multifactorial diseases such as Graves' orbitopathy and craniofacial abnormalities, like Apert's syndrome.^[4,31] Needless to say, adequate information of the orbital cavity is essential for surgeons to demarcate safe surgical areas and minimize the risk of damage to neurovascular structures during orbital procedures.^[32] Unfortunately, in clinical practice, orbital volume changes are often evaluated qualitatively and subjectively, rather than with a standardized quantitative and objective fashion. The primary limitation behind this adequate management is that most volumetric procedures are time laborious and time-consuming and often prone to erroneous calculation, based on the grader's experience. Optimized stereological method has been proposed as an alternative technique which can significantly lower the required manual work. It has been studied before in different organs using MRI and CT.^[33-37]

To the knowledge of the authors, this is the first *ex vivo* study to demonstrate the applicability of both planimetry and stereology in measuring the orbital volume on MR datasets as opposed to previous cadaver studies.^[38] A limitation of this study is that the applied semi-automated methodologies require appropriate software and user training. An operational system using a fully automated algorithm for precise orbital volume measurements should be targeted in future research.

CONCLUSION

In this article, we evaluated planimetry and stereology for orbital volumetry using MRI, with a view to eliminate subjective bias. The optimized stereological method can provide reproducible orbital volume estimates from a series of MR images with the minimum user intervention. However, our experiments clearly revealed that the optimized stereological method might lead to a mean difference exceeding 1 cc from the real orbital volume. The above difference is sometimes unacceptable in clinical practice. Planimetric measurements performed by users with good knowledge of the orbital anatomy as depicted on MR images can improve the accuracy of the obtained volumetric results. The laborious manual planimetry may be considered as the method of choice for highly accurate orbital volume measurements from MRI data.

Financial support and sponsorship

This study has received funding by the General Secretariat for Research and Technology (GSRT) and the Hellenic Foundation for Research and Innovation (HFRI).

Conflicts of interest

There are no conflicts of interest.

REFERENCES

1. Alinasab B, Beckman MO, Pansell T, Abdi S, Westermarck AH, Stjärne P. Relative difference in orbital volume as an indication for surgical reconstruction in isolated orbital floor fractures. *Craniomaxillofac Trauma Reconstr* 2011;4:203-12.
2. Heller RS, David CA, Heilman CB. Orbital reconstruction for tumor-associated proptosis: Quantitative analysis of postoperative orbital volume and final eye position, *Journal of Neurosurgery* 2019;132:927-32.
3. Haskins CP, Nurkic S, Fredenburg KM, Dziegielewski PT, Mendenhall WM. Primary orbital melanoma treated with orbital exenteration and postoperative radiotherapy: A case report and review of the literature. *Head Neck* 2018;40:E17-20.
4. Imai K, Fujimoto T, Takahashi M, Maruyama Y, Yamaguchi K. Preoperative and postoperative orbital volume in patients with Crouzon and Apert syndrome. *J Craniofac Surg* 2013;24:191-4.
5. Gellrich NC, Schramm A, Hammer B, Rojas S, Cufi D, Lagrèze W, *et al.* Computer-assisted secondary reconstruction of unilateral posttraumatic orbital deformity. *Plast Reconstr Surg* 2002;110:1417-29.

6. Oh TS, Jeong WS, Chang TJ, Koh KS, Choi JW. Customized orbital wall reconstruction using three-dimensionally printed rapid prototype model in patients with orbital wall fracture. *J Craniofac Surg* 2016;27:2020-4.
7. Weaver AA, Loftis KL, Tan JC, Duma SM, Stitzel JD. CT based three-dimensional measurement of orbit and eye anthropometry. *Invest Ophthalmol Vis Sci* 2010;51:4892.
8. Watanabe M, Buch K, Fujita A, Jara H, Qureshi MM, Sakai O. Quantitative MR imaging of intra-orbital structures: Tissue-specific measurements and age dependency compared to extra-orbital structures using multispectral quantitative MR imaging. *Orbit* 2017;36:189-96.
9. Kainz HI, Bale R, Donnemiller E, Gabriel M, Kovacs P, Decristoforo C, *et al.* Image fusion analysis of 99m Tc-HYNIC-octreotide scintigraphy and CT/MRI in patients with thyroid-associated orbitopathy: The importance of the lacrimal gland. *Eur J Nucl Med Mol Imaging* 2003;30:1155-9.
10. Yao X, Chaganti S, Nabar KP, Nelson K, Plassard A, Harrigan RL, *et al.* Structural-functional relationships between eye orbital imaging biomarkers and clinical visual assessments. In: Styner MA, Angelini ED, editors. *Proceedings of SPIE-the International Society for Optical Engineering*. 2017. p. 101331.
11. Forbes G, Gehring D, Gorman C, Brennan M, Jackson I. Volume measurements of normal orbital structures by computed tomographic analysis. *Am J Roentgenol* 1985;145:149-54.
12. McGurk M, Whitehouse RW, Taylor PM, Swinson B. Orbital volume measured by a low-dose CT scanning technique. *Dentomaxillofac Radiol* 1992;21:70-2.
13. Lutzemberger L, Salvetti O. Volumetric analysis of CT orbital images. *Med Biol Eng Comput* 1998;36:661-6.
14. Deveci M, Öztürk S, Şengezer M, Pabuşcu Y. Measurement of orbital volume by a 3-dimensional software program: An experimental study. *J Oral Maxillofac Surg* 2000;58:645-8.
15. Detorakis ET, Drakonaki E, Papadaki E, Pallikaris IG, Tsilimbaris MK. Effective orbital volume and eyeball position: An MRI study. *Orbit* 2010;29:244-9.
16. Erkoç MF, Öztoprak B, Gümüş C, Okur A. Exploration of orbital and orbital soft-tissue volume changes with gender and body parameters using magnetic resonance imaging. *Exp Ther Med* 2015;9:1991-7.
17. Warfield SK, Kaus M, Jolesz FA, Kikinis R. Adaptive, template moderated, spatially varying statistical classification. *Med Image Anal* 2000;4:43-55.
18. Mazonakis M, Karampekios S, Damilakis J, Voloudaki A, Gourtsoyiannis N. Stereological estimation of total intracranial volume on CT images. *Eur Radiol* 2004;14:1285-90.
19. Unal B, Kara A, Aksak S, Unal D. A stereological assessment method for estimating the surface area of cycloids. *Eurasian J Med* 2010;42:66-73.
20. Gundersen HJ, Jensen EB. The efficiency of systematic sampling in stereology and its prediction. *J Microsc* 1987;147:229-63.
21. Bilgic S, Sahin B, Sonmez OF, Odaci E, Colakoglu S, Kaplan S, *et al.* A new approach for the estimation of intervertebral disc volume using the Cavalieri principle and computed tomography images. *Clin Neurol Neurosurg* 2005;107:282-8.
22. Bontzos G, Mazonakis M, Papadaki E, Maris TG, Blazaki S, Drakonaki EE, *et al.* *Ex vivo* orbital volumetry using stereology and CT imaging: A comparison with manual planimetry. *Eur Radiol* 2019;29:1365-74.
23. Tsiapa I, Tsilimbaris MK, Papadaki E, Bouziotis P, Pallikaris IG, Karantanas AH, *et al.* High resolution MR eye protocol optimization: Comparison between 3D-CISS, 3D-PSIF and 3D-VIBE sequences. *Phys Med* 2015;31:774-80.
24. Koh E, Walton ER, Watson P. VIBE MRI: An alternative to CT in the imaging of sports-related osseous pathology? *Br J Radiol* 2018;91:1088.
25. Roberts N, Puddephat MJ, McNulty V. The benefit of stereology for quantitative radiology. *Br J Radiol* 2000;73:679-97.
26. Mazonakis M, Damilakis J, Varveris H. Bladder and rectum volume estimations using CT and stereology. *Comput Med Imaging Graph* 1998;22:195-201.
27. Neuschwander TB, Chang EL, Sadun AA. Hertel curve: Orbital volume increment and proptosis in a cadaver model. *Ophthal Plast Reconstr Surg* 2005;21:431-4.
28. Sung YS, Chung CM, Hong IP. The correlation between the degree of enophthalmos and the extent of fracture in medial orbital wall fracture left untreated for over six months: A retrospective analysis of 81 cases at a single institution. *Arch Plast Surg* 2013;40:335-40.
29. Ahn HB, Ryu WY, Yoo KW, Park WC, Rho SH, Lee JH, *et al.* Prediction of enophthalmos by computer-based volume measurement of orbital fractures in a Korean population. *Ophthalmic Plast Reconstr Surg* 2008;24:36-9.
30. Dubois L, Steenen SA, Gooris PJ, Mourits MP, Becking AG. Controversies in orbital reconstruction—I. Defect-driven orbital reconstruction: A systematic review. *Int J Oral Maxillofac Surg* 2015;44:308-15.
31. Shen J, Jiang W, Luo Y, Cai Q, Li Z, Chen Z, *et al.* Establishment of magnetic resonance imaging 3D reconstruction technology of orbital soft tissue and its preliminary application in patients with thyroid-associated ophthalmopathy. *Clin Endocrinol (Oxf)* 2018;88:637-44.
32. Danko I, Haug RH. An experimental investigation of the safe distance for internal orbital dissection. *J Oral Maxillofac Surg* 1998;56:749-52.
33. Sadeghi A, Asghari H, Hami J, Mohasel Roodi M, Mostafae H, Karimipour M, Namavar M, *et al.* Volumetric investigation of the hippocampus in rat offspring due to diabetes in pregnancy-A stereological study. *J Chem Neuroanat* 2019;101:101669.
34. Taman FD, Kervancioglu P, Kervancioglu AS, Turhan B. The importance of volume and area fractions of cerebellar volume and vermian subregion areas: A stereological study on MR images. *Childs Nerv Syst* 2020;36:165-71.
35. Sahin B, Emirzeoglu M, Uzun A, Incesu L, Bek Y, Bilgic S, *et al.* Unbiased estimation of the liver volume by the Cavalieri principle using magnetic resonance images. *Eur J Radiol* 2003;47:164-70.
36. Mazonakis M, Stratakis J, Damilakis J. Efficient stereological approaches for the volumetry of a normal or enlarged spleen from MDCT images. *Eur Radiol* 2015;25:1761-7.
37. Manios GE, Mazonakis M, Voulgaris C, Karantanas A, Damilakis J. Abdominal fat volume estimation by stereology on CT: A comparison with manual planimetry. *Eur Radiol* 2016;26:706-13.
38. Acer N, Sahin B, Ergür H, Basaloglu H, Ceri NG. Stereological estimation of the orbital volume: A criterion standard study. *J Craniofac Surg* 2009;20:921-5.